Nanoscale

ROYAL SOCIETY OF CHEMISTRY

MINIREVIEW

View Article Online
View Journal | View Issue

Cite this: *Nanoscale*, 2025, **17**, 12048

A review on the insights into redox-based regeneration strategies for $LiFePO_4$ batteries

Junhui Cai, Yanjuan Li,* Shengnv Xu, Yiran Li, ZhanZhan Wang, Jie Liu, Shun Yang * and Xiao Yan *

In recent years, the market share of lithium iron phosphate ($LiFePO_4$: LFP) batteries within the power battery sector has witnessed substantial growth. In light of low-carbon initiatives and environmental sustainability, the recycling of spent $LiFePO_4$ (SLFP) batteries, especially their regeneration, is of paramount importance for environmental protection, resource conservation, and enhancement of economic efficiency. Current literature reviews predominantly concentrate on synthesizing existing research from the perspective of regeneration methodologies. However, they insufficiently address the chemical reactions that are integral to the regeneration process, which are essential for optimizing the recycling of SLFP batteries. To address this gap in the literature, this review, for the first time, systematically compiles studies from the innovative perspective of redox reactions occurring during the regeneration of SLFP batteries. This review commences with an analysis of the economic benefits and failure mechanisms linked to the regeneration of SLFP batteries, thereby elucidating the rationale and necessity for this process. Subsequently, it delves into indirect regeneration methods based on oxidation reactions and direct regeneration technologies based on reduction reactions. Furthermore, the review underscores research dedicated to the enhancement and repurposing of SLFP battery cathodes, offering a prospective outlook on the novel trends in the recycling of SLFP battery materials. This review aspires to promote further scholarly inquiry into the regeneration of SLFP batteries.

Received 8th November 2024,
Accepted 12th April 2025

DOI: 10.1039/d4nr04671d

rsc.li/nanoscale

Introduction

The advancement of societies and the expansion of economies have resulted in an increased global demand for sustainable energy.[1–3] To mitigate carbon emissions and achieve carbon neutrality, nations are actively seeking alternative energy sources to supplant conventional fossil fuels.[4–6] Lithium-ion batteries (LIBs) have become prevalent in powering vehicles and facilitating energy storage owing to their high capacity and extended cycle life.[7–11] In 2023, the global sales of electric vehicles approached 14 million units, representing an increase of 3.5 million units from 2022, which is an annual growth of 35 per cent,[12] as shown in Fig. 1a. Projections indicate that it

School of Chemistry & Materials Science, Jiangsu Normal University, Xuzhou, 221116, China. E-mail: yanxiao@jsnu.edu.cn

Junhui Cai

Junhui Cai received his Bachelor's degree in Chemistry specialty (pedagogical) from Jiangsu Normal University of Technology. He is carrying out his Master's degree research at Jiangsu Normal University under the supervision of Prof. Xiao Yan. Currently, his research focuses on the recycling of spent lithium-ion batteries.

Xiao Yan

Xiao Yan received his PhD degree in Physics from Jilin University in 2014. He joined Jiangsu Normal University in 2016 His research interests include recycling spent lithium-ion batteries and high-energy secondary batteries.

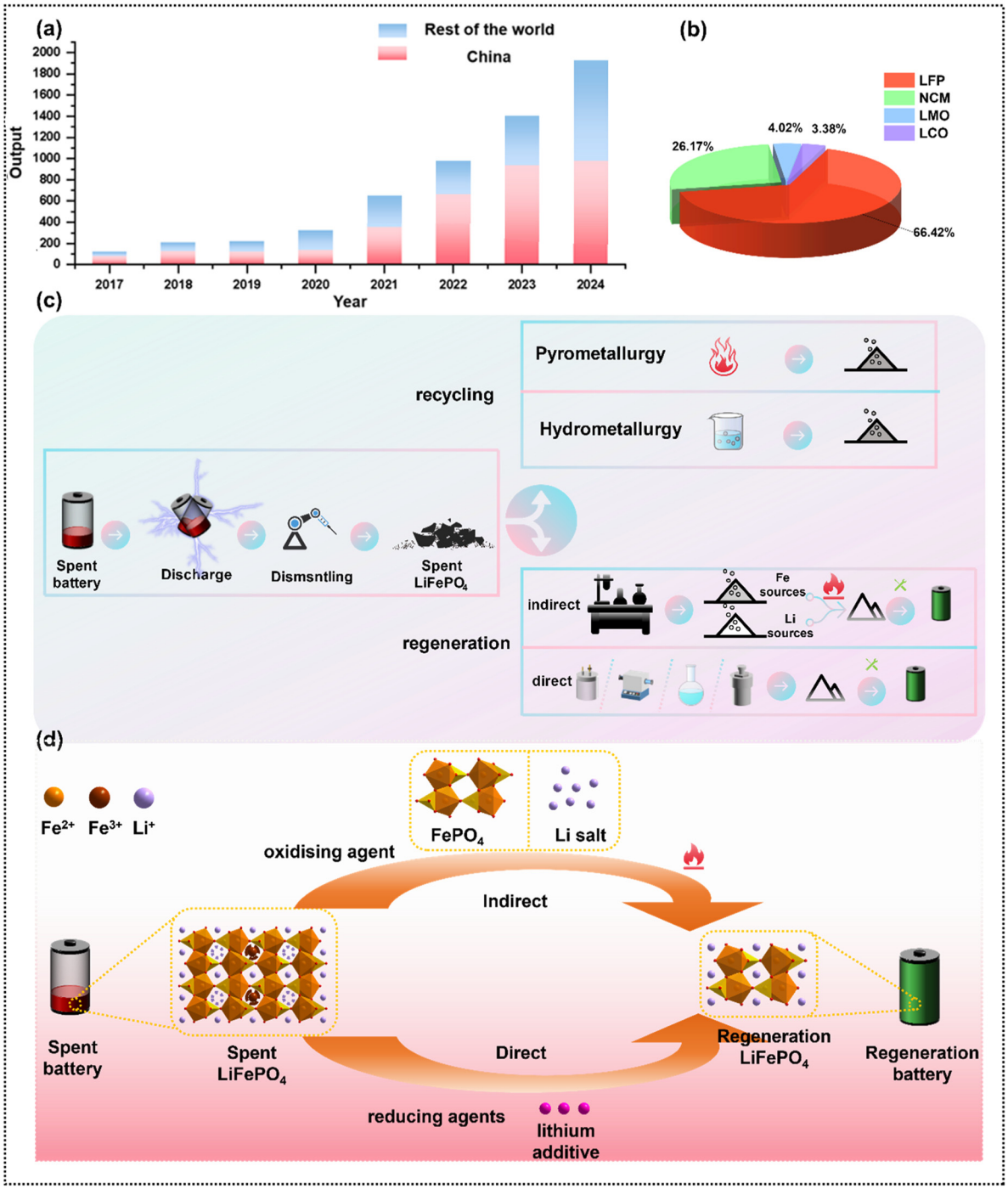

Fig. 1 (a) Electric vehicle production in China and other countries since 2017 (b) proportion of lithium-ion battery cathode materials shipped to China (c) recycling and regeneration process of SLFP batteries (d) scheme of regeneration mechanism for LFP cathode materials.

may reach around 17 million units by 2024, accounting for more than one-fifth of global vehicle sales. As the service life of electric vehicle power batteries ranges from five to eight years, early new energy vehicle batteries have already entered the end-of-life period, and the scale of the end-of-life batteries market will continue to increase with the process of electrification. Various countries have repeatedly modified the primary categories of power batteries with the advancements in these batteries. For instance, in China, the predominant types of power batteries have transitioned from lithium iron phosphate (LFP) to ternary cathode materials (NCM) and back to LFP. Prior to 2017, LFP was predominantly installed in the domestic renewable energy vehicles.[13] Since 2017, China has revised its subsidy policy for new energy vehicles to incorporate the

energy density of batteries as a criterion for subsidy eligibility. Consequently, the subsidies for low-density LFP batteries have been reduced, as these batteries no longer meet the subsidy standards. In contrast, high energy density NCM batteries are being increasingly promoted. According to statistics from the Power Battery Industry Innovation Alliance, NCM batteries surpassed LFP batteries in market share after 2018, exceeding 60% in 2020. The freezing of the energy density index after 2021 resulted in the gradual development with LFP, and the proportion using this type of power battery is gradually increasing. Nowadays, LFP is the mainstream type of installed power battery. In March 2023, the installed capacity of LFP has reached 69%. Currently, the battery recycling market remains at a developmental stage similar to that of five years prior. As LFP batteries enter their decommissioning phase, they are anticipated to constitute the majority of recyclable batteries. The peak of the growth rate of the LFP battery recycling business is in the distant future. Projections reveal that the LFP power battery recycling market space could expand to a value of 56.7 billion by 2027, with the 2024–2026 period for LFP battery recycling market space representing high growth.

Compared to other parts of the battery, the recycling of LFP cathode materials offers the most favorable economic viability for recycling. The main recycling methods are divided into pyrometallurgy and hydrometallurgy (Fig. 1b).[14–17] The main research direction is to improve the recovery rate of lithium as much as possible.[18–21] Since 2022, the price of lithium carbonate continues to be at a high level, with the recycling value more economical, so the current market for the pricing of spent $LiFePO_4$ (SLFP) batteries basically only considers the value of lithium. Compared to NCM batteries, the current LFP recycling technology and the development of the recycling market are relatively insufficient.[22] Although the proportion of iron phosphate is significantly higher compared to lithium metal, the recovery of iron phosphate from LFP is challenging, resulting in limited economic benefits. Consequently, the market has historically perceived the recycling of LFP batteries as economically unviable, leading to a relatively small number of enterprises engaging in lithium iron recycling. Compared with traditional pyrometallurgical and hydrometallurgical recycling of waste lithium iron phosphate batteries, direct recycling offers significant economic benefits,[23–25] considering the costs of recycling and regeneration in terms of energy consumption, chemical reagents, environmental protection, and so on (additional Table 1). Direct regeneration usually costs much less than recycling and offers higher profits,[26] which can improve the entire battery closed-loop recycling system. In summary, although LFP battery recycling presents economic potential, there are numerous challenges and bottlenecks that must be overcome. It is undeniable that considerable economic potential exists behind these challenges and bottlenecks. However, LFP batteries are currently primarily utilized in a step-by-step manner due to its stable structure and high safety advantages.[27–29] LFP batteries in new energy vehicles with an attenuation of more than 20% will not be able to meet the requirements of car driving, indicating that the battery needs to be recycled. Decommissioned batteries with an attenuation interval of 20%–40% can meet the requirements of secondary use, such as in the communication base station, solar street lamps, UPS power supply and other small energy storage areas. An attenuation of more than 40% is generally taken in the way of recycling, dismantling for the sale of materials. LFP regeneration research has gradually become the current research hotspot by comprehensively considering the nature of LFPs and the economic value of recycling.[30,31] Regeneration of lithium iron phosphate has a very promising future from an economic and environmentally friendly point of view. A number of scholars have conducted research in this area, and some reviews have been published. In the existing research, researchers summarize the classification or battery regeneration, such as pyrometallurgical, hydrometallurgical and other methods.[32,33] However, these approaches merely serve as auxiliary means of regeneration, especially in regeneration methods. To enhance exploration and optimize the regenerating SLFP battery cathode materials, it is imperative to synthesize existing studies from a more fund amential perspective.

In this review, we systematically compile reported studies from the innovative perspective of the redox reactions occurring during the regeneration of SLFP batteries (Fig. 1c and d). The regeneration process can be categorized into two distinct types based on the underlying reaction mechanisms: indirect regeneration based on oxidation reactions and direct regeneration based on reduction reactions.[34,35] In the indirect regeneration process, adding oxidizing agents to elevate the valence of Fe in SLFP battery cathode materials facilitates the maximal extraction of lithium and enables the effective separation of lithium and iron, resulting in the formation of compounds such as Li_2CO_3 and $FePO_4$. Subsequently, these compounds are utilized in the synthesis of regenerated $LiFePO_4$ (RLFP) cathode materials. However, the unavoidable oxidation separation process may lead to secondary environmental pollution,

Table 1 Cost comparison of different regeneration processes

	Pyrometallurgical ($ per t)	Hydrometallurgical ($ per t)	Regeneration ($ per t)
Pretreatment	~46	~120	~77
Chemical agent	~123	~460	~185
Energy consumption	~538	~307	~123
Equipment depreciation	~231	~185	~92
Environmentally friendly treatment	~307	~230	~62
Total cost	~1290	~1302	~539

and the treatment process is complicated and consumes a lot of energy, resulting in higher costs. On the other hand, the direct regeneration method selects a suitable reductant to directly reduce the Fe(III) occupying the Li-site in the SLFP battery to Fe(II) to reduce the Li–Fe anti-site defects and repair its structure.[36,37] Direct regeneration obviates the necessity for the leaching process, thereby enhancing its environmental sustainability and energy efficiency compared with indirect regeneration. This method can effectively regenerate and restore its original electrochemical properties, but also upgrade and modify the anode material, resulting in improved performance.[38,39]

Based on a comprehensive review of recent research on LFP regeneration, a promising direction for future investigations into the regeneration of SLFP batteries has been identified. This direction is crucial for advancing the understanding of the regeneration mechanism of SLFP batteries.

Failure mechanisms of LFP cathodes

Compositional failure

The major cause of capacity degradation in LFP cathode materials after long-term cycling is lithium (Li) loss which will result in inducing partial formation of lithium vacancy (Fig. 2a). Peng *et al.*[40] demonstrated that lithium defects in the cycled LFP reached 47.1% after 6500 cycles. Furthermore, the decomposition of lithium hexafluorophosphate ($LiPF_6$) in the electrolyte occurs under conditions of trace water or elevated temperatures and leads to the formation of hydrofluoric acid (HF). The presence of HF corrodes the surface of the LFP cathode, thereby facilitating the dissolution of iron within the material's structure. This process directly results in the degradation of cathode active material and induces structural phase change, whereby Fe ions dissolved into the electrolyte are unevenly deposited on the surface of the negative electrode and indirectly catalyse the excessive growth of SEI, leading to a loss of active lithium, attenuation of the overall battery capacity and increased impedance. Fu *et al.*[41] investigated the electrochemical performance of LFP//graphite batteries at 25, 45 and 65 °C over 2000 cycles. Their study demonstrated that aged batteries exhibit an activation period and a linear decay period exists in the aged battery at 25 and 45 °C, while an additional accelerated decay period exists at 65 °C. The findings indicate that the principal mechanism contributing to capacity degradation in LFP//graphite batteries under conditions of temperature-accelerated aging due to elevated temperatures is the depletion of active lithium reserves. The losses of inactive lithium were classified into three distinct categories: inorganic solid-electrolyte interphase (SEI), organic SEI, and Li_xC_6. Among these, inorganic SEI is identified as the predominant factor in capacity loss.

Structural failure

The deintercalation/intercalation mechanism in LFP cathodes involves a two-phase transition process between LFP of the rhombohedral crystal system and iron phosphate of the hexagonal crystal system. Upon completion of the charging process, the cell volume of $FePO_4$ decreases by 6.77% compared to that of LFP.[42–44] During the long-term cycling process of the battery, the recurrent expansion and contraction of the cell induces compressive stress accumulation within the particles, which subsequently leads to the formation of dislocations and other material defects.[45–48] The eventual large-scale release of this compressive stress will directly cause a wide range of particles to crack, which is macroscopically manifested as a sudden decrease in the electrode's electronic conductivity.

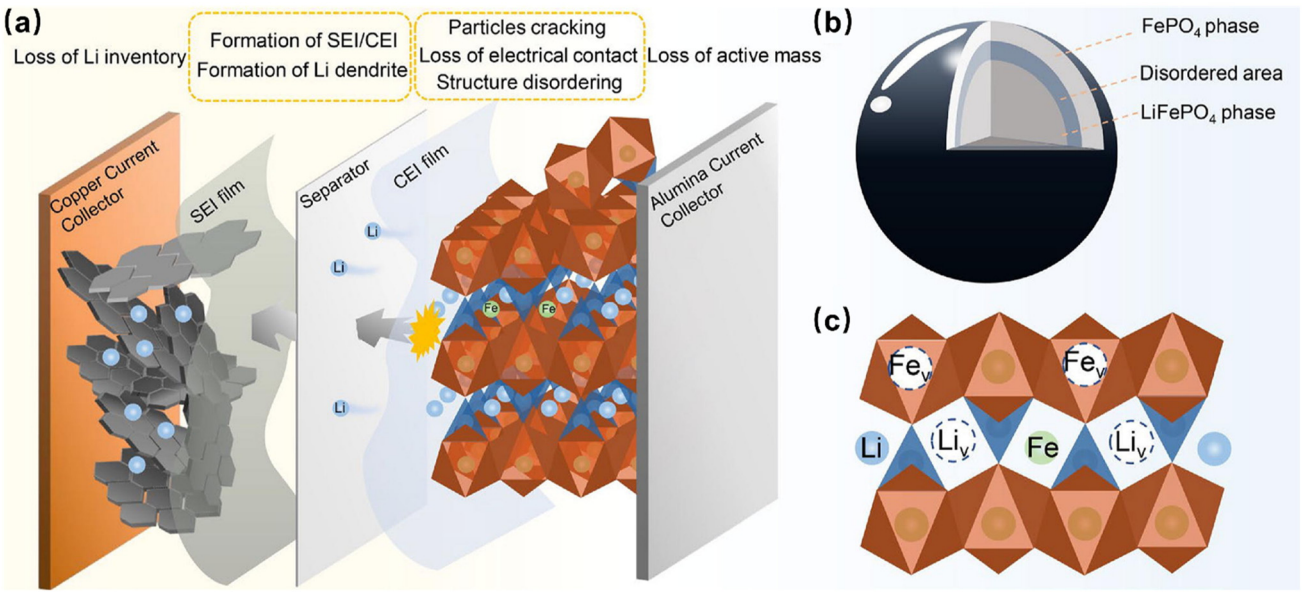

Fig. 2 (a–c) Degradation mechanism of LFP cathode materials. Reproduced from ref. 17, Copyright 2024, with permission from Elsevier.

Another cause of structural failure is an antisite defect (Fe occupying Li sites) within LFP, which can have an impact on the performance of the battery. Since lithium-ion transport within $LiFePO_4$ is one-dimensional, the presence of such defects can impede the movement of lithium ions.[29,49] Furthermore, these defects can cause destabilization of the LFP structure due to the increased electrostatic repulsion introduced by the high valence state (Fig. 2b and c).

Surface-interface issues

Thermally unstable decomposition byproducts of $LiPF_6$ in the electrolyte will form a cathode electrolyte interphase (CEI) layer on the surface of LFP. In variable application environments, high-temperature cycling accelerates the increase of LiPF6 oxide byproducts in the electrolyte, resulting in cathodic interface failure.[50]

In conclusion, the essential approach to rejuvenating LFP cathode materials involves addressing the depletion of active lithium ions and reestablishing the stable structure of LFP. Currently, the predominant restoration techniques are categorized into two primary strategies based on their regeneration methodologies: indirect regeneration and direct regeneration. The following sections provide a detailed overview of these two strategies.

Indirect regeneration based on oxidation reaction

Based on the battery discharge mechanism, Fe^{2+} in the LFP crystal undergo oxidation to Fe^{3+} by the oxidant, with the diffusion of Li^+ ions out of the crystal lattice. Consequently, the introduction of an oxidant into the solution during the regeneration process facilitates the selective release of embedded Li^+ ions from the LFP cathode material. This process facilitates the efficient separation and recovery of lithium and iron. Subsequently, the SLFP battery material can be regenerated by supplementing with lithium salts as a precursor. The present study focuses on identifying the suitable oxidizing agents and reaction methods for the green and efficient separation and recovery of Li and Fe. By judiciously selecting a suitable oxidizing agent, the generation of waste and pollutants in the recovery process can be minimized. Furthermore, optimizing redox reactions could reduce energy consumption and enhance recovery energy efficiency.

Oxidizing agent-H_2O_2

Hydrogen peroxide is a common oxidizing agent used in the hydrometallurgical recovery process of LFP since it is green and inexpensive. In the selective leaching process, the addition of a precise quantity coupled with the regulation of solution pH facilitates the presence of lithium in the liquid phase as Li^+. Concurrently, iron and phosphorus are sequestered as $FePO_4$ precipitate. This methodology enables the efficient recycling of lithium and reduces energy costs and environmental pollution. H_2O_2 is commonly used with acids or alone.

In an acidic environment, Fe^{2+} is oxidized to Fe^{3+}, forming iron phosphate ($FePO_4$), and lithium is dissolved from LFP to form Li^+, which can be precipitated as lithium salt by subsequent treatment. The above obtained lithium salt and $FePO_4$ were used to regenerate LFP:

$$LiFePO_4 + \text{acid} + H_2O_2 \rightarrow Li^+ + FePO_4 + H_2O \quad (1)$$

$$\text{Lithium salt} + FePO_4 \rightarrow LiFePO_4. \quad (2)$$

The selective leaching process will be shortened to one step of leaching and separation, which has received widespread attention and subsequent research. Li *et al.*[19] was the first to propose adding hydrogen peroxide as an oxidant to assist sulfuric acid leaching, and the results showed a high selectivity and leaching rate: the lithium leaching rate reached 96.85%, while the iron leaching rate was only 0.027%.

Chen *et al.*[51] developed a decontamination method using mixed bases to extract lithium, analyzing the effectiveness of strong and weak bases at the same pH. Initially, Li^+ and $FePO_4$ were selectively extracted from an SLFP battery using low concentrations of H_2SO_4 and H_2O_2. Then, NaOH and $NH_3{\cdot}H_2O$ were used to purify the extracted Li^+-containing liquid, and sodium carbonate was used to precipitate Li_2CO_3. The RLFP using Li_2CO_3 (99.51%) and $FePO_4$ as raw materials showed an initial discharge capacity of 126.7 mA h g^{-1} and retained 98.02% capacity after 100 cycles at 0.5 C.

Carbon coating is the most commonly used way to further enhance the electrochemical performance of RLFP.[52] Fu *et al.*[53] used the H_2SO_4–H_2O_2 system to leach LFP powder, optimized the leaching process conditions, and the leaching rate of lithium and iron elements reached 98.79% and 94.97%, respectively. Glucose was added as a carbon source in the subsequent process of RLFP, and the final LFP/C material regenerated at 700 °C had excellent electrochemical performance, with a first discharge specific capacity of 160.1 mA h g^{-1} at 0.1 C.

Zhou *et al.*[54] added the SLFP powder into the combined treatment solution of NaH_2PO_4 and H_2O_2 for the oxidative leaching reaction (Fig. 3a and b). The lithium leaching rate was 98.65% and the iron leaching rate was only 0.028%, which produced Li_3PO_4 and $FePO_4$. The RLFP showed excellent multiplicity performance and long-term cycling stability. To promote environmentally sustainable recycling and regeneration practices, a novel green and efficient regeneration process devoid of acids and alkalis have been developed for SLFP batteries. This process is based on an oxidative leaching reaction and has been successfully implemented to regenerate cathode materials. In the oxidative leaching process, H_2O_2 functions as both an oxidizing and reducing agent. Part of it is dedicated to oxidizing Fe(II), while the remainder executes the reduction reaction. Efficient leaching of lithium can be achieved by appropriately adjusting or controlling the leaching parameters, realizing the conversion of high-purity lithium carbonate and iron phosphate. Qiu *et al.*[55] utilized this method to achieve a 97.6% leaching rate of lithium to regenerate the cathode material (Fig. 3c). The final RLFP maintained a capacity of 144 mA h g^{-1} at 1 C, with a capacity loss of less

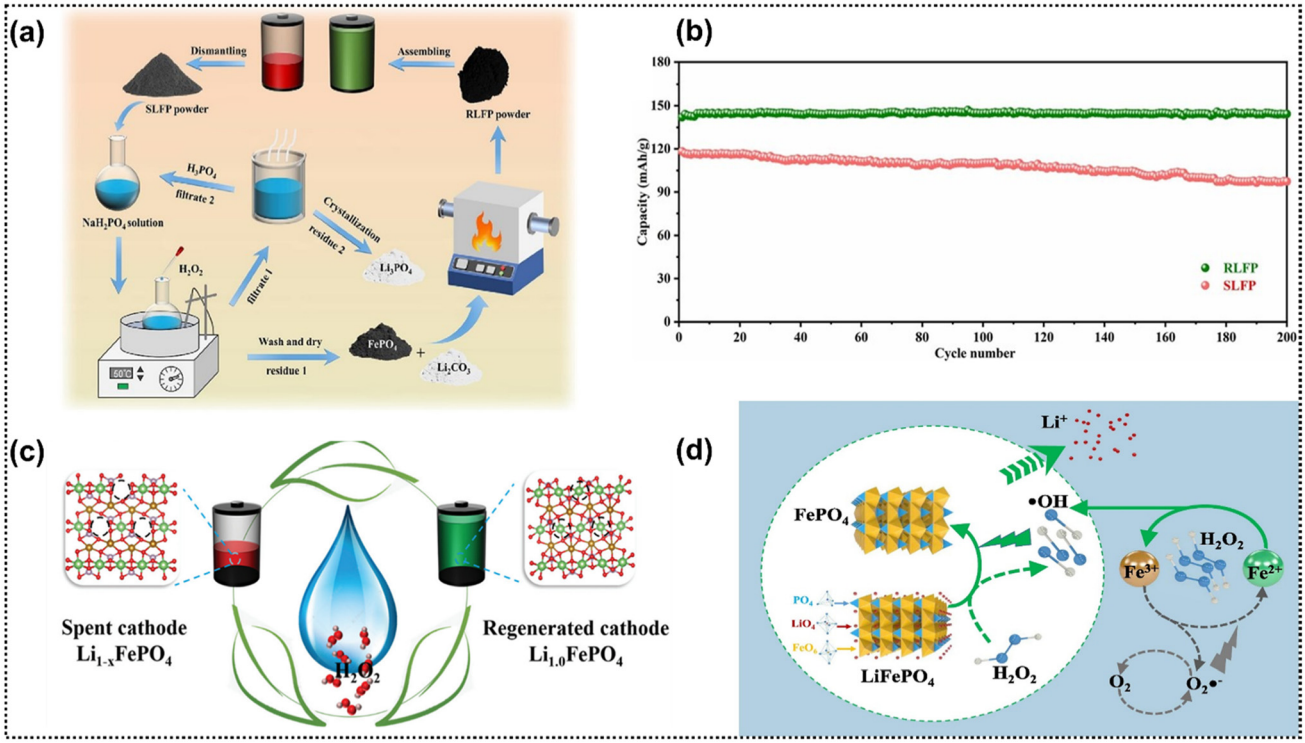

Fig. 3 (a) Flowchart of recycling and regeneration of SLFP battery cathode powder. Reproduced from ref. 54, Copyright 2023, with permission from Elsevier. (b) Long-term performance of SLFP and RLFP batteries at 0.5 C for 200 cycles. Reproduced from ref. 54, Copyright 2023, with permission from Elsevier. (c) Schematic of the regeneration of RLFP cathode materials *via* hydrogen peroxide leaching. Reproduced from ref. 55, Copyright 2022, with permission from the Royal Society of Chemistry. (d) Schematic of the detailed transformation of different products for the *in situ* recycling of $FePO_4$ and Li^+ *via* advanced oxidation metallurgy. Reproduced from ref. 57, Copyright 2023, with permission from Elsevier.

than 1% after 100 cycles, which provides excellent multiplication capability and long-term cycling stability. Xu *et al.*[56] directly decomposed the positive electrode into aluminum foil a high-purity $FePO_4$ and lithium-containing solution, in which the leaching efficiency of Li was more than 96.3% and the impurities were scarce. The RLFP had a discharge capacity of 137.1 mA h g^{-1} at 1 C after 250 cycles, with almost no capacity loss, showing excellent electrochemical performance and the ability to meet the requirements for secondary utilization.

Hydrogen peroxide also provides the intermediate oxidizing species required for the reaction. The mechanism suggests that the oxidation of Fe(II) and the release of Li^+ from LFP are mainly triggered by the rapid attack of a large amount of –OH during advanced oxidation according to DFT calculations and chemical reaction analyses. The released Li^+ is recycled as Li_2CO_3 and used as a precursor for the remanufacture of LFP together with $FePO_4$. Chen *et al.*[57] innovatively proposed an *in situ* advanced oxidative metallurgy method to selectively extract lithium from LFP by Fenton oxidation instead of the conventional metallurgical process (Fig. 3d). Li can be completely released without destroying the olive-type structure of LFP and form the $FePO_4$ precursor. The RLFP showed excellent electrochemical performance with a first discharge capacity of 138.9 mA h g^{-1} at 0.5 C and a capacity retention of 93.6% after 50 cycles.

Oxidizing agent-persulfate

Persulfate (MS_2O_8) is a commonly used oxidizing agent for the regeneration of SLFP battery cathode materials because it is solid at room temperature and soluble in water. Persulfate has a wider range of applications compared with hydrogen peroxide. It is suitable for hydrometallurgical regeneration and can be used in traditional thermal regeneration:

$$2LiFePO_4 + MS_2O_8 = 2FePO_4 + MSO_4 + Li_2SO_4. \quad (3)$$

Zhang *et al.*[58] devised a thermal oxidation strategy to extract lithium from an SLFP battery using a hot phase process and synergistically controlled melt oxidation of sulfate under oxygen atmosphere. The desired conversion of LFP to soluble lithium salts and $FePO_4$ was achieved while maintaining the initial morphology of the particles with the following reaction:

$$2LiFePO_4 + (NH_4)_2S_2O_8 + O_2 = 2FePO_4 + Li_2SO_4 + 2NH_3 + 2H_2O \quad (4)$$

Thermodynamic and DFT calculations confirmed the feasibility of lithium precipitation from molten salt. The RLFP showed excellent electrochemical performance with a discharge capacity of 136.2 mA h g^{-1} at 1 C and a capacity retention of 98.9% after 100 cycles.

Sun *et al.*[59] proposed that the selective extraction and recovery of lithium from LFP cells could be achieved using only $NH_4S_2O_8$ as the oxidizing and leaching agent (Fig. 4a). Over 99% of lithium was selectively extracted, while the olivine skeleton of $FePO_4$ remains intact after oxidative leaching (Fig. 4b).

This route does not include inorganic or organic acid leaching, complex pH adjustment and waste water treatment processes. After optimizing the process conditions, Li_2CO_3 and $FePO_4$ can be recovered with a recovery rate of more than 96%, and the RLFP cathode has the electrochemical performance with a discharge capacity of 163.9 mA h g^{-1} at 0.1 C and 120 mA h g^{-1} at 4 C. After 100 cycles of 0.2 C, the capacity retention rate is 98.0% (Fig. 4c).

Chen *et al.*[60] investigated and proposed a carbothermal reduction technique for the regeneration of LFP using the recycled raw materials from SLFP batteries to further improve the electrochemical performance of the RLFP, in which Li_2CO_3 recovered from the SLFP battery served as the lithium source, and $FePO_4$ provided the iron and phosphorus sources. The application of a carbon coating facilitated more intimate particle contact, reduced the Li^+ diffusion pathway within LFP, and enhanced the electronic and ionic conductivity. Optimal electrochemical performance was achieved with a carbon coating mass fraction of 12 wt% in the RLFP material. It has a high specific discharge capacity of 146.89 mA h g^{-1} at 1 C and an excellent capacity retention of 97.9% after 200 cycles. In addition, it has satisfactory capacity retention of 96.1% and 94.3% at 2 C and 5 C, respectively (Fig. 4d).

Oxidizing agent-O_2

In contrast to the aforementioned methods, an alternative indirect regeneration strategy involves fire pretreatment. This approach entails the direct oxidation of Fe to iron oxide by calcining the SLFP battery materials in air, thereby completely disrupting the original structure to facilitate lithium–iron separation. Concurrently, this method effectively removes certain impurities present in the cathode materials, including PVDF, conductive carbon, and aluminum. Subsequently, SLFP battery is regenerated through the addition of a lithium source, among other components. Chen *et al.*[61] first explored the direct thermal treatment of recycled cathode powder at different temperatures. The recycled powder could be effectively restored and reused for lithium-ion batteries after high-temperature treatment at 650 °C. The researchers further explored the reaction mechanism. Li *et al.*[62] employed a novel approach combining pre-oxidation and a granulation-based co-coating method to regenerate a severely degraded SLFP battery. The pre-oxidation process effectively decomposed the binder and residual carbon, resulting in the conversion of lithium and iron into $Li_3Fe_2(PO_4)_3$ and Fe_2O_3, respectively. The subsequent regeneration process involved the addition of lithium carbonate to synthesize spherical LFP co-coated with carbon and Li_3PO_4 (Fig. 5a). The electrochemical performance of the regenerated material was comparable to that of commercial LFP. Wang *et al.*[63] developed a direct regeneration method of LFP based on a doping strategy (Fig. 5b). Initially, the SLFP battery was oxidized in a high-temperature oxygen environ-

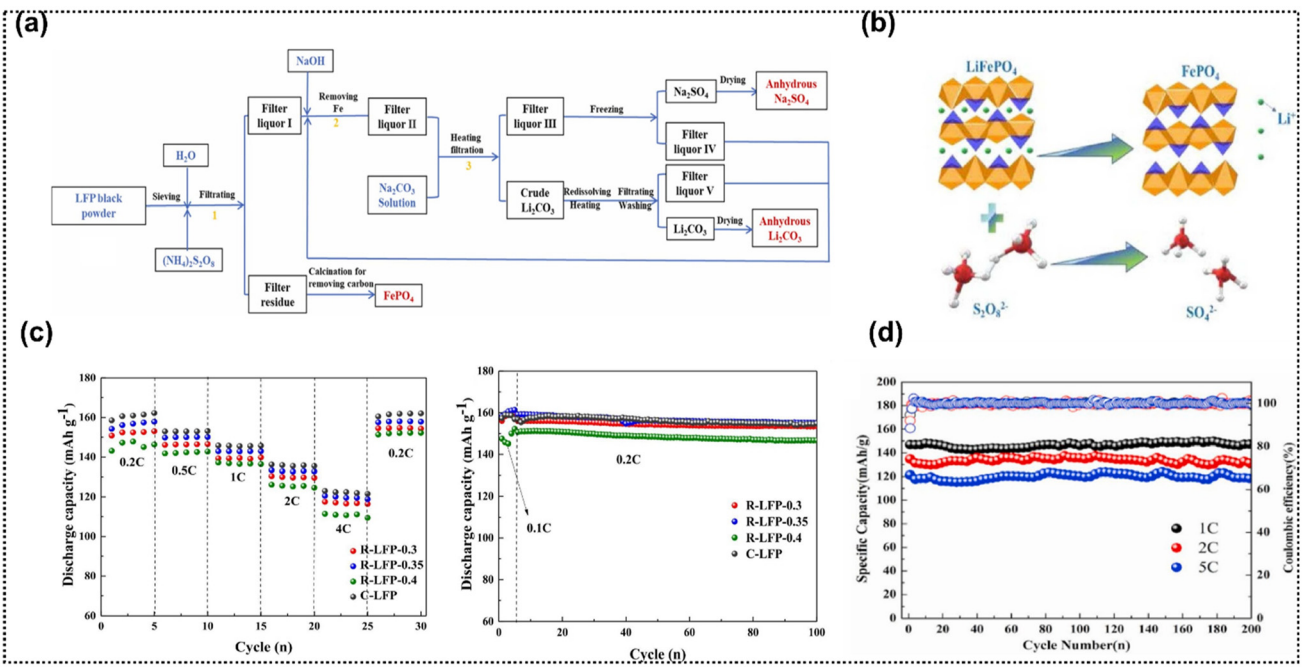

Fig. 4 (a) Flow chart of the recovery of Li_2CO_3 and $FePO_4$ from SLFP black powder. Reproduced from ref. 59, Copyright 2023, with permission from Elsevier. (b) Schematic of the reaction between $LiFePO_4$ and $(NH_4)_2S_2O_8$. Reproduced from ref. 59, Copyright 2023, with permission from Elsevier. (c) RLFP rate performance and cycling stability at 0.1 C and 0.2 C. Reproduced from ref. 59, Copyright 2023, with permission from Elsevier. (d) Cyclic performance of sample RLFP at 1 C, 2 C, and 5 C. Reproduced from ref. 60, Copyright 2022, with permission from Elsevier.

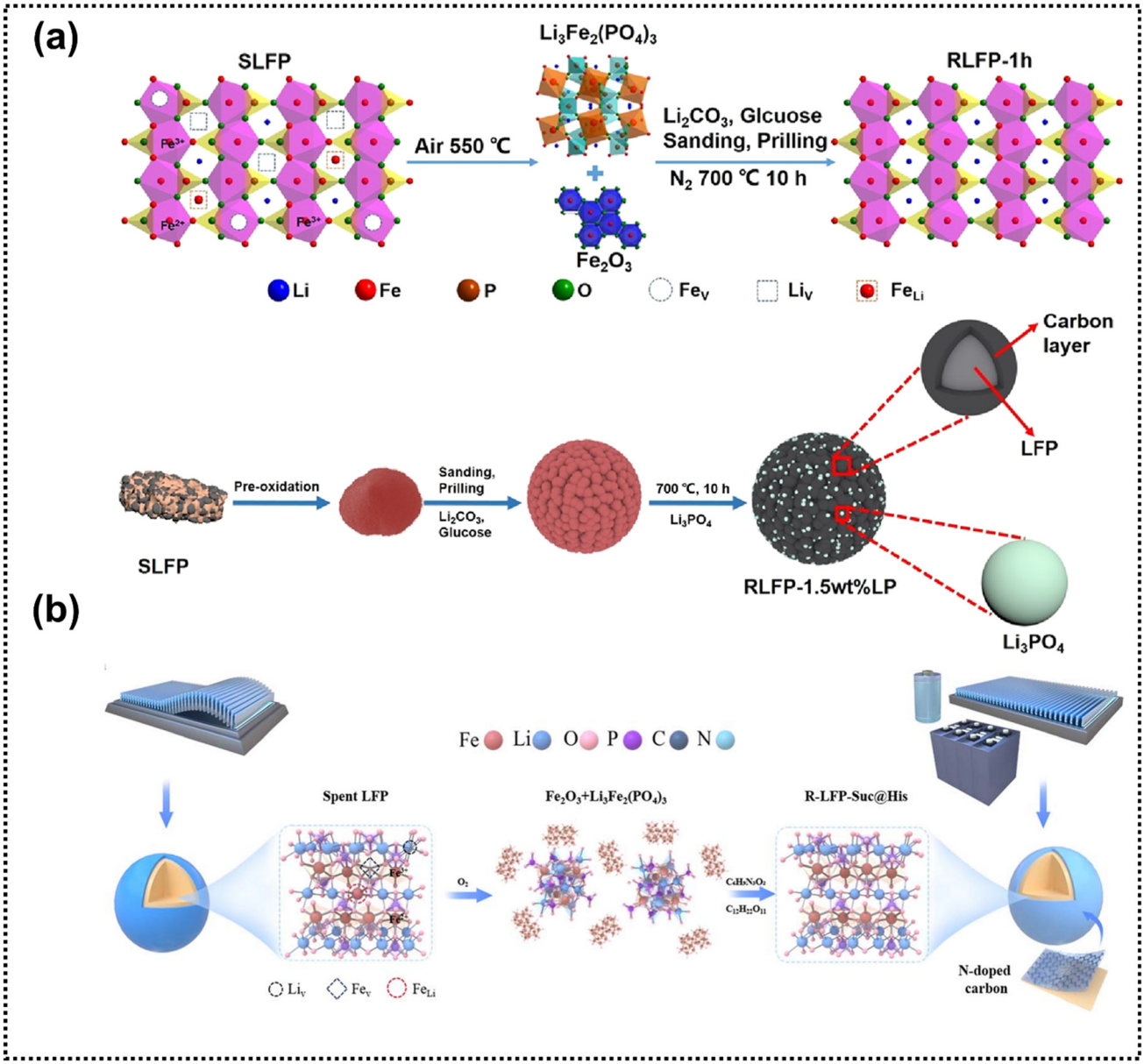

Fig. 5 (a) Schematic of cooperative RLFP. Reproduced from ref. 62, Copyright 2024, with permission from the American Chemical Society. (b) Schematic of the regeneration of SLFP batteries. Reproduced from ref. 63, Copyright 2024, with permission from the Royal Society of Chemistry.

ment. Then, sucrose and glycine were added to prevent Fe ion migration and enhance Li^+ and electron diffusion by forming a nitrogen-doped carbon coating. The RLFP cathode demonstrated excellent cycling stability, retaining 98.7% capacity after 100 cycles at 1 C and 87.9% after 500 cycles at 1 C.

Electrochemical indirect oxidation

Electrochemical indirect oxidation involves the generation of oxidizing intermediates during the electrolysis process. These oxidizing agents are either attached to electrode surfaces or dispersed in the solution, where they facilitate the oxidation of target substances. This process can occur at the anode and cathode.[64] Indirect electrolysis can be achieved at positive and negative potentials that are lower than those required for direct electron transfer at the electrode through the use of a homogeneous electron transfer medium. Indirect electrolysis can be performed at reduced positive and negative potentials using a homogeneous electron transfer medium compared with the higher potentials needed for direct electron transfer at the electrode. This leads to reduced energy consumption, enhanced reaction energy efficiency, decreased electron transfer overpotential, and avoidance of direct electrolysis limitations.[65] The process of indirect oxidation primarily depends on the production of potent oxidizing agents to oxidize the Fe^{2+} ions in LFP. The leaching process closely resembles a homogeneous reaction, facilitating complete interaction

between LFP and the oxidizing agents without necessitating elevated temperatures to enhance LFP dispersion. The utilization of electrons as environmentally friendly oxidants minimizes the need for additional chemical reagents, thereby supporting the efficient recovery of lithium products in subsequent stages.

Tian *et al.*[66] developed an electrochemical system employing a boron-doped diamond (BDD) electrode with a high oxygen evolution potential as the anode and RuO_2/Ti as the cathode to produce oxidizing species and enhance oxidative reaction contact for the indirect oxidation of LFP. This innovative approach facilitates efficient and rapid selective leaching of lithium and iron ions through indirect oxidation, thereby achieving selective leaching while substantially minimizing reaction time. Zhang *et al.*[67] used a low-cost sodium chloride solution as the electrolyte, Pt as the cathode and graphite as the anode. In the electrochemical LFP regeneration reactor, the Cl^-/ClO^- pair that is generated electrochemically in NaCl solution is adopted as the redox mediator to break down LFP into $FePO_4$ and Li^+ *via* the redox targeting reaction without extra chemicals. The RLFP cathode material was regenerated from recycled Li_2CO_3 and $FePO_4$ and offers enhanced electrochemical performance and excellent cycling stability.

In summary, the indirect regeneration strategy for LFP relies on the oxidation reaction, which can preferentially and selectively leach lithium with high efficiency, but the leaching residue requires additional processing. Simultaneous leaching of all elements from SLFP battery materials allows for the extraction of valuable components in a single step and may result in lithium loss. Meanwhile, simultaneous leaching of all elements from SLFP battery materials allows for the extraction of valuable components in one step, which complicates the separation process and may lead to lithium loss. Consequently, indirect regeneration methods are often characterized by a prolonged recovery process and the production of substantial quantities of waste liquid. This method does not provide economic benefits, particularly for LFP materials that do not contain expensive metals (*e.g.*, cobalt). Additionally, although the profile regeneration recovers lithium and iron, respectively, during regeneration, it remains essential to adjust the lithium-to-iron ratio appropriately to synthesize new LFP material.

This adjustment may necessitate the addition of supplementary lithium or iron sources, thereby diminishing economic efficiency. Therefore, current researchers are committed to further improving the lithium leaching efficiency, while environmental protection is an even more significant issue for them to consider. Table 2 summarizes the effect of different oxidizers on the yield of lithium iron phosphate and the performance of regenerated batteries.

Direct regeneration based on reduction reaction

In recent years, a strategy of direct regeneration of LFP has been proposed. This approach is informed by the failure mechanism of LFP and aims to address two critical aspects to achieve successful regeneration. First, it is necessary to restore the structure of Fe(III), which occupies the position of Li, back to Fe(II) through the addition of reducing agents. Secondly, the appropriate selection of lithium salts is necessary to replenish the deficient active lithium and restore its capacity. Among these considerations, the most crucial is the repair of the LFP structure, underscoring the importance of selecting suitable reducing agents and strategies.

Inorganic reducing agents

Inorganic reductants have the advantages of lower cost and easy availability of raw materials, which are usually synergized with an auxiliary strategy to regenerate LFP. Current research focuses on inorganic reductants that are environmentally friendly, low in dosage, and functional. Jing *et al.*[70] first used N_2H_4–H_2O as a reductant and adopted a one-step hydro-

Table 2 Comparison of various indirect regeneration methods for LFP materials

Oxidising agent	Recovery of Li (%)	Recovery of Fe (%)	Regeneration additives	Electrochemical performance	Ref.
H_2SO_4–H_2O_2	98.79	94.97	Glucose	160.1 mA h g^{-1} at 0.1 C and capacity retention of 99.7% after 100 cycles at 1 C	53
$NH_4S_2O_8$	96	—	Glucose	163.9 mA h g^{-1} at 0.1 C, 120 mA h g^{-1} at 4 C and capacity retention ratio of 98.0% after 100 cycles at 0.2 C	59
$NH_4S_2O_8$	>99	—	Glucose	136.2 mA h g^{-1} at 1 C and 98.9% capacity retention after 100 cycles	58
NaH_2PO and H_2O_2	98.65	—	Glucose	144.3 mA h g^{-1} at 0.5 C and 99% capacity retention after 200 cycles	54
Fe(II)–H_2O_2	99.9	—	Glucose	138.9 mA h g^{-1} at 0.5 C and 93.6% capacity retention after 50 cycles	57
H_2SO_4–H_2O_2	99.51	—	—	126.7 mA h g^{-1} at 0.5 C and 98.02% capacity retention after 100 cycles	51
$NH_4S_2O_8$	97.06	—	—	154.2 mA h g^{-1} at 0.5 C and 91.0% capacity retention after 300 cycles at 1 C	68
$NH_4S_2O_8$	—	—	Glucose	146.89 mA h g^{-1} at 1 C and 97.9% capacity retention after 200 cycles	60
H_2O_2	96.3	—	Glucose	137.1 mA h g^{-1} at 1 C after 250 cycles with almost no capacity loss	56
H_2O_2	97.6	—	Citric acid	144 mA h g^{-1} at 1 C with less than 1% capacity loss after 100 cycles	55
H_2O_2	99.9	97.5	Glucose	144.2, 139.0, 133.2, 125.5, and 110.5 mA h g^{-1} at 0.1, 0.5, 1, 2, and 5 C	69
O_2	—	—	Sucrose	138.8 mA h g^{-1} at 1 C and 98.7% capacity retention after 100 cycles	63
O_2	—	—	—	155.7 mA h g^{-1} at 0.1 C and it remained at 149.2 mA h g^{-1} after 100 cycles	62
ClO^-	99.70%	99.15%	—	114.6 mA h g^{-1} at 5 C and 94.0% capacity retention after 300 cycles	67

thermal method to regenerate the SLFP battery, confirming the feasibility of N_2H_4–H_2O as a reductant for SLFP regeneration. However, researchers later used other auxiliary strategies to regenerate SLFP batteries since the hydrothermal method is hard to apply in industry. N_2H_4–H_2O is a commonly utilized reducing agent to reduce Fe(III) back to Fe(II) and then lithium salt was added to repair lithium vacancy defects and antisite defects and consequently regenerate LFP.

Song *et al.*[71] employed N_2H_4–H_2O as a reducing agent and LiCl as a lithium source to address lithium vacancy defects and antisite defects in SLFP batteries. This was achieved through the application of ultrasound, which facilitated the generation of localized high temperatures, high pressures, and intense shock wave jets (Fig. 6a). The RLFP has a discharge specific capacity of 135.1 mA h g^{-1} after 100 cycles at a current density of 1 C, with a capacity retention rate as high as 97%. The reaction product of N_2H_4–H_2O is mainly N_2, which is environmentally friendly. To enhance energy efficiency and safety, researchers revisited a low-temperature liquid lithium replenishment strategy using N_2H_4–H_2O as a reducing agent and LiCl as a lithium source.[72] This method replenishes missing Li^+ ions and reduces antisite defects through annealing, restoring nearly all lost Li^+ ions at 80 °C over 6 h (Fig. 6b). Subsequent annealing removed the Li^+ ions and electrochemical evaluation showcased the outstanding properties of RLFP-80 °C/6 h.

Wang *et al.*[73] proposed a simple recrystallization method by reacting an SLFP battery cathode material with $LiNO_3$ (Fig. 6c). Benefiting from the thermodynamic instability and low melting point of $LiNO_3$ (~250 °C), the SLFP battery was completely relithiated by heating in air at 300 °C (just below the LFP melting point (~250 °C) of $LiNO_3$, the SLFP battery was completely relithiated by heating in air at 300 °C (just below the LFP oxidation temperature) for 30 min. The specific capacity of the repaired LFP was restored from 134 mA h g^{-1} to 162 mA h g^{-1}, with improved specific capacity and cycling performance comparable to that of commercial new LFP. However, harmful NO_2 gas is generated in the process, which is not environmentally friendly enough.

Reductive lithium-containing substances as a bifunctional additive are also used to achieve Li compensation while reducing Fe^{3+}, which has the advantages of low energy consumption and good environment. For instance, the regeneration mechanism using LiI is as follows:

$$Li_{1-x}FePO_4 + xLiI = LiFePO_4 + 1/2xI_2 \quad (5)$$

Ouaneche *et al.*[74] reported that LFP can be efficiently recovered by optimizing the experimental parameters using direct lithiation of LiI in ethanol solution, which is one of the greenest and cheapest solvents, without any additional heat treatment (Fig. 6d). The RLFP has excellent electrochemical performance: the first turn capacity is 168 mA h g^{-1} at 0.1 C and the coulombic efficiency of 25 cycles exceeds 98%.

In addition to inorganic solids, gaseous atmospheres with reducing properties can also be effective in regenerating LFP. Sun *et al.*[75] roasted discarded LFP cathodes in CO_2 to partially remove carbon coatings, then used mechanical milling to mix the lithium source with LFP. The CO_2 reacted with the carbon, creating a reducing atmosphere that converted Fe^{3+} to Fe^{2+}, decreasing the Fe^{3+} content. The improved pretreatment method more effectively restored the crystal structure of SLFP

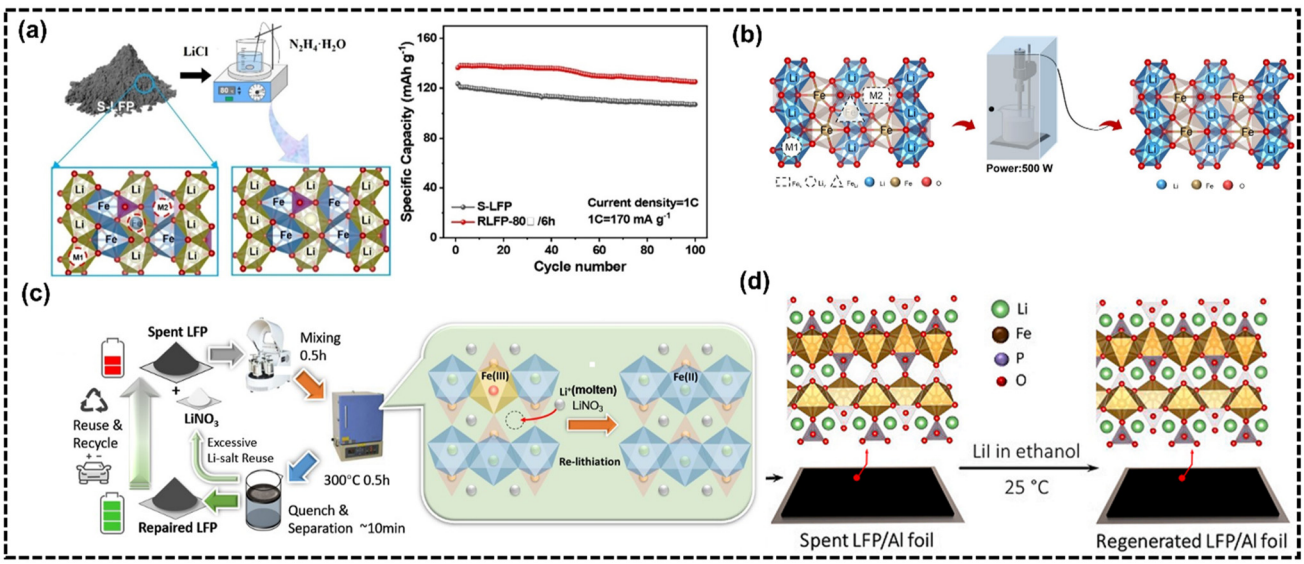

Fig. 6 (a) LFP battery regeneration enhanced *via* an eco-friendly N_2H_4–H_2O method, restoring Li ions and reducing defects and the comparison of cycle performance before and after regeneration. Reproduced from ref. 71, Copyright 2024, with permission from Elsevier. (b) Flowchart of the regeneration of an SLFP battery cathode powder. Reproduced from ref. 72, Copyright 2024, with permission from Elsevier. (c) Schematic of the SLFP battery repairing procedures. Reproduced from ref. 73, Copyright 2023, with permission from the Royal Society of Chemistry. (d) SLFP battery regenerated at room temperature *via* DCL. Reproduced from ref. 74, Copyright 2023, with permission from Elsevier.

battery cathode material, resulting in excellent electrochemical performance and cycling stability, with an initial capacity of 149.1 mA h g^{-1} at 0.1 C. Compared with the traditional pretreatment method, the crystal structure of the SLFP battery cathode material was repaired more completely, and the RLFP material showed good electrochemical performance and cycling stability. The initial capacity could reach 149.1 mA h g^{-1} at 0.1 C.

Organic reducing agents

Compared with inorganic reductants, organic reductants can effectively form a carbon coating layer during the regeneration process, which can effectively regenerate LFP, further optimize the conductive network of LFP and improve its electrochemical performance. The selection of a suitable organic reductant combined with a suitable lithium source for direct regeneration of LFP is a hotspot in current research.[76,77]

Glucose is an extremely common and easily available organic material that is often used as a carbon source in the indirect regeneration of LFP. In the direct regeneration process, glucose can be used as a carbon source, but more importantly as a reducing agent to reduce Fe^{3+} to Fe^{2+} to achieve the repair of the structure of the SLFP battery and to achieve a uniform layer of carbon coating, which optimizes the electrical conductivity of the cathode material. The main reaction process is as follows:

$$Li_{1-x}FePO_4 + C_6H_{12}O_6 + xLi^+ = LiFePO_4 + 6C + 6H_2O \quad (6)$$

Han *et al.*[78] extracted SLFP battery cathode materials from SLFP batteries using pyrolysis and flotation. They adjusted the Li to Fe ratio with lithium carbonate, used glucose as a reducing agent, and calcined the mixture at 650 °C under argon for 11 h. The regenerated $LiFePO_4$/C achieved an initial discharge capacity of 161.88 mA h g^{-1} and retained 157.89 mA h g^{-1} after 100 cycles, demonstrating strong electrochemical and cycling performance. Ascorbic acid is a more commonly used organic reductant, with advantages of effective reducing ability and compatibility with aqueous systems. Song *et al.*[79] directly regenerated LFP using a high-power ultrasonic liquid-phase reaction with ascorbic acid as the reducing agent and LiOH as the lithium source (Fig. 6a), where $C_6H_6O_6$ was produced by the reaction of ascorbic acid without the regenerated LFP surface. Its electrochemical performance was more general since it formed an effective carbon coating.

Heteroatom participation and the construction of high-performance carbon cladding layers are usually employed in the regeneration process of organic reductants to achieve better electrochemical performance of the regenerated LFP, such that the carbon cladding layer can effectively enhance the conductivity of the cathode material and the stability of the overall structure.[80–82] For example, Mao *et al.*[83] used ascorbic acid as the reductant and LiOH as the lithium source to regenerate LFP using an ultrasonic-assisted method (Fig. 7b). The subsequent introduction of graphene regenerated from the negative electrode by electrostatic self-assembly helps to form a layered structure and conductive network for the RLFP (Fig. 7c), thus realizing the rapid ion and electron transfer of the redox reaction. When doped with 5 wt% graphene, the specific capacity of the regenerated LFP/MWrGO composites was increased to 161.4 mA h g^{-1}, with a capacity retention of 94.9% at 0.2 C. Zhou *et al.*[84] used the solution mixture with NaCl salt as the template for pore creation which undergoes an "ice and fire" process: ice drying helps to embed the NaCl into the glucose coating on the LFP particles, and annealing (carbonization) at 650 °C induces the conversion of glucose from an electron donor into a unique 3D porous carbon network between the RLFP nanoparticles (Fig. 7d). The reconfiguration of the porous channels provided convenient access for lithium-ion transport and electrolyte penetration. The RLFP achieved reversible capacities of 169.74 and 141.79 mA h g^{-1} at 0.1 C and 1 C, respectively, with a retention rate of over 95.7% at 1 C after 200 cycles.

In addition to constructing a unique carbon network, heteroatom doping can effectively improve the stability of the carbon layer and enhance the ion diffusion performance. Cheng *et al.*[85] regenerated an SLFP battery by hydrothermal treatment and sintering using ethanol as solvent and reducing agent and lithium acetate (CH_3COOLi) as lithium source (Fig. 7e). The destruction of LFPs generally starts from the surface, so inhibiting the destruction of the LFP's adjacent surfaces plays a key role in preventing the LFP's destruction of LFP as a whole. A heterogeneous interface was constructed between the nitrogen-doped carbon (NC) obtained by adding polyvinylpyrrolidone (PVP) and the regenerated LFP. The cycling stability of the regenerated LFP (RSLFP@NC) was improved by introducing N atoms to regulate the position of the d-band center of Fe near the anode surface.

Melamine is a wise selection to reduce the amount of pharmaceuticals and improve the economic efficiency. The reduction of Fe^{3+} to Fe^{2+} was favored by doping using melamine with a certain reducing property. More importantly, the N atoms contained in melamine itself are doped into the carbon layer through C–N bonds, forming carbon-doped LFP composites without the need of adding additional carbon sources. Jin *et al.*[86] regenerated an SLFP battery and repaired the battery performance by adding lithium carbonate and melamine under heat treatment conditions (Fig. 7f). The RLFP also exhibited excellent capacity retention up to 99.03% after 200 cycles and excellent multiplicative performance with a discharge capacity of 116 mA h g^{-1} at 5 C. The systematic study demonstrated that the nitrogen-doped carbon coating plays a crucial role in improving the performance of the RLFP cathode material.

Cheng *et al.*[87] advanced the process by using a multifunctional organolithium salt (3,4-dihydroxybenzonitrile dilithium) that acts as a reductant, Li source, and carbon source to directly regenerate discarded LFP cathodes (Fig. 7g). The organolithium salt's functional groups bond with RLFP, lithium fills vacancies, and cyano creates a reducing atmosphere to prevent the Fe(III) phase. Additionally, salt pyrolysis forms an

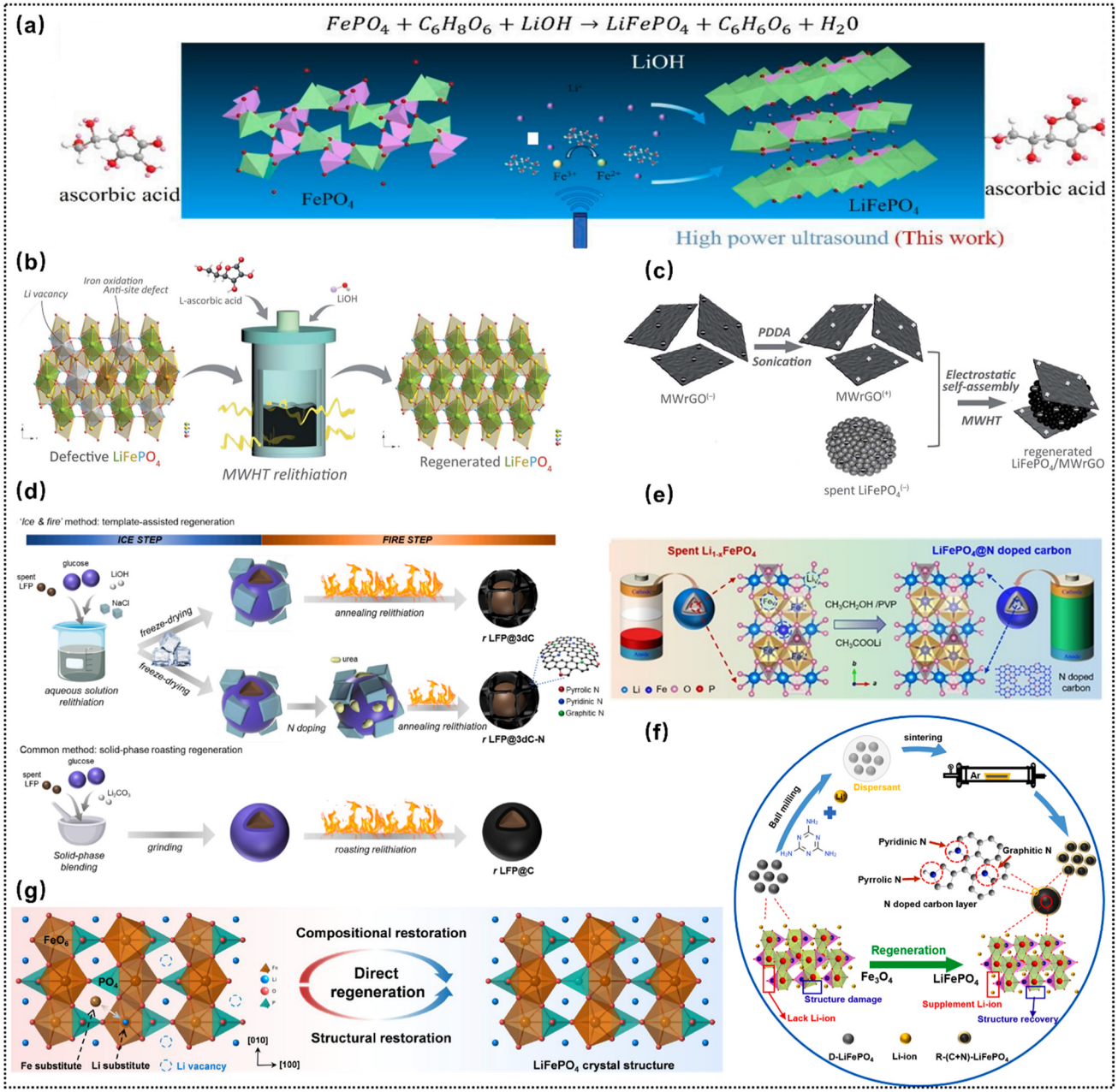

Fig. 7 (a) Schematic showing the methodology of high-power sonication using ascorbic acid as the reducing agent and LiOH as the lithium source. Reproduced from ref. 79, Copyright 2024, with permission from Elsevier. (b) Microwave-hydrothermal (MWHT) regenerating process. Reproduced from ref. 83, Copyright 2021, with permission from the Royal Society of Chemistry. (c) Composition of the transition state between SLFP and MWrGO during the MWHT regenerating process. Reproduced from ref. 83, Copyright 2021, with permission from the Royal Society of Chemistry. (d) Workflow diagram of 'ice and fire' two-step method *via* template-assisted regeneration and common solid-phase roasting method. Reproduced from ref. 84, Copyright 2023, with permission from Elsevier. (e) Schematic of the direct regeneration of SLFP battery. Reproduced from ref. 85, Copyright 2022, with permission from Wiley. (f) Preparation process of R-(C + N)-$LiFePO_4$. Reproduced from ref. 86, Copyright 2024, with permission from Elsevier. (g) Schematic of the degraded and restored crystal structures. Reproduced from ref. 85, Copyright 2023, with permission from Springer Nature.

amorphous conductive carbon layer on the LFP particles. Based on the mechanism of LFP regeneration, the regeneration of SLFP battery cathode materials can be achieved under room temperature conditions with a suitable reducing agent and supplementation of an appropriate lithium source. Inspired by room temperature lithiation, Zhang *et al.*[88] tried to regenerate the whole cathode directly without stripping off the cathode material, and the triethyl lithium borohydride/tetrahydrofuran solution was used as a lithium replenishment agent and a reductant to achieve the direct regeneration of

cathode material. Direct regeneration of the cathode material eliminates the need for separation, regeneration, and electrode remanufacturing processes, reduces total energy consumption by 80%, and increases revenues by 53% compared with traditional direct regeneration. This method is environmentally and economically competitive and is a very interesting direction for future research.

Reducing agent-electron(e^-)

Electrochemical reduction mainly relies on electrons as a reducing agent to directly reduce Fe(III) to Fe(II), which is very environmentally friendly. In this process, lithium ions in the lithium salt aqueous solution are driven to the empty space of the degraded cathode through the potential difference on the electrode, and the RLFP is subsequently obtained through a short annealing process. Huang *et al.*[89] first put forward the targeted electrically driven lithiation, achieving low-temperature repair of lithium iron phosphate. The regenerated material has a discharge capacity of 135.2 mA h g^{-1} at 1 C and a capacity retention rate of 95.3% after 500 cycles, confirming the feasibility of electrochemical regeneration of lithium iron phosphate.

Wu *et al.*[90] proposed a re-lithiation approach that intercalates lithium ions into scrapped LFP in an aqueous solution system. Specifically, Fe(III) was reduced by electrons acting as a reducing agent, while Li in the lithium salt solution acted as a Li source to replenish the missing Li in the SLFP. The RLFP exhibits excellent electrochemical performance with a high discharge capacity of 134.0 mA h g^{-1} at 1 C. In order to further reduce the use of additives, Wang *et al.*[91] proposed an ingenious electrochemical method with simultaneous anodic delithiation/cathodic lithium-embedded regeneration to regenerate an SLFP battery. The SLFP was charged/discharged in an electrolytic system, where it was used as the anode and the cathode ($Li_xFePO_4|Li_2SO_4|Li_xFePO_4$). The electrolysis process does not require an external Li source and the identical material of the cathode and anode could reduce the theoretical voltages for Li embedding and de-embedding, thus reducing energy consumption.

Yang *et al.*[92] proposed a nondisassembly repair strategy for degraded cells through a lithium restoration method based on deep discharge, which can elevate the anodic potential to result in the selective oxidative decomposition and thinning of the SEI on the graphite anode. Both the electron and lithium sources required for the reductive regeneration of SLFP batteries come from the oxidative decomposition of the SEI.

Current research in direct regeneration has progressively shifted toward shortened-process methodologies characterized by low-energy-consumption profiles and enhanced environ-

Table 3 Comparison of various direct regeneration methods for LFP materials

Reducing agent and additives	Lithium salt	Strategy	Electrochemical performance	Ref.
Chitin and graphene oxide	LiOH	Repeated freezing and thawing, spray-drying	124.8 mA h g^{-1} at 2 C, 117.5 mA h g^{-1} at 5 C, and 149.7 mA h g^{-1} at 0.2 C	95
CO	Li_2CO_3	High-temperature calcination	149.1 mA h g^{-1} at 0.1 C	75
$N_2H_4{\cdot}H_2O$	LiCl	Low-temperature liquid-phase and high-temperature sintering	146.45 mA h g^{-1} at 1 C and 92% capacity retention after 100 cycles	72
Ascorbic acid	LiOH	High power ultrasonic reactions	154.71 mA h g^{-1} at 0.1 C and 93.56% capacity retention after 200 cycles at 1 C	79
Melamine	Li_2CO_3	High-temperature calcination	168 mA h g^{-1}, 156 mA h g^{-1} and 151 mA h g^{-1} at 0.05 C, 0.2 C and 1 C, respectively	86
$N_2H_4{\cdot}H_2O$	LiCl	High power ultrasonic reactions	135.1 mA h g^{-1} and 97% capacity retention after 100 cycles at 1 C	71
Glucose	LiOH	Solution-based relithiation and high-temperature sintering	169.74 and 141.79 mA h g^{-1} at 0.1 and 1 C, respectively and a > 95.7% retention rate at 1 C after 200 cycles	84
LiI	LiI	Direct lithiation in solution	160 mA h g^{-1} at 1 C,	74
$LiNO_3$	$LiNO_3$	recrystallization	162 mA h g^{-1} at 0.1 C, and 90% capacity retention after 500 cycles	73
Na_2SO_3	Li_2SO_4	Hydrothermal	145.1, 142.7, 139.9, 135.9, and 129.3 mA h g^{-1} at 0.1,0.2, 0.5, 1, 2, and 5 C, respectively and >99% capacity retention after 100 cycles at 1 C	96
3,4-Dihydroxybenzonitrile dilithium	3,4-Dihydroxybenzonitrile dilithium	High-temperature calcination	157 mA h g^{-1}, 127, 111, and 97 mA h g^{-1} at 0.1, 2, 5 and 10 C, respectively	87
Glucose	Li_2CO_3	Flotation process after effective pyrolysis	161.37 mA h g^{-1} at 0.1 C and 97.53% capacity retention after 100 cycles at 0.2 C	78
Ascorbic acid	Li_2CO_3	Spray drying and high-temperature solid-phase method	160 mA h g^{-1} at 0.1 C and 80% capacity retention after 800 cycles at 1 C	97
CH_3CH_2OH	CH_3COOLi	Hydrothermal	~80% capacity retention after 1000 cycles at 10 C	85
Ascorbic acid	LiOH	Microwave-reduced	161.4 mA h g^{-1} at 0.2 C and 94.9% capacity retention after 100 cycles	80
Tartaric acid	LiOH	Hydrothermal	165.9, 151.93, 145.92, 133.11 and 114.96 mA h g^{-1} at 0.1, 0.5, 1, 2, and 5 C, respectively	98
e^-	SEI	Electrochemical	Stable cycling for 300 cycles at 1 C	91

mental compatibility. Although numerous regeneration strategies employ brief annealing processes to improve crystallinity and structural stability of regenerated materials, this approach inevitably prolongs procedural complexity and escalates energy expenditure. Consequently, emerging research focuses on developing post-annealing-free regeneration protocols to optimize process efficiency. This paradigm shift necessitates stringent requirements for reducing agent selection and precise control over ambient condition during the redox-driven reconstruction phase.[93] As demonstrated by Wu *et al.*[94] in their electrochemical regeneration protocol for SLFP batteries, well-crystallized RLFP was successfully synthesized by applying a controlled electrolytic current of 5 mA, achieving structural reconstruction without requiring post-annealing treatment. Electrochemical regeneration shows that adjusting the current can regulate the crystallinity of RLFP, enhancing its electrochemical performance. However, other regeneration methods require further investigation into their mechanisms to achieve efficient, closed-loop regeneration with low energy consumption. Direct regeneration streamlines the process compared with indirect regeneration, enhancing environmental sustainability, and significantly reducing costs, yielding economic and ecological advantages. The use of suitable lithium salts and reduction additives facilitates the regeneration of SLFP batteries more rapidly and with reduced energy consumption. Current perspectives on multifunctional organic lithium salts suggest that, besides restoring lithium and structural integrity, they also contribute to the formation of an effective carbon coating layer. This approach is economically more viable than the addition of lithium source and reductant, with a very good prospect for development. Therefore, more multifunctional reducing agents and reducing processes with lower costs will be the mainstream of future development for the direct regeneration of lithium iron phosphate. Table 3 summarized the effect of different reductants and reduction method on the performance of regenerative batteries.

Conclusion and outlook

LFP has emerged as a significant commercial battery technology following extensive research and application. In the foreseeable future, the disposal of SLFP batteries present a critical issue requiring urgent resolution. To achieve more environmentally friendly and efficient disposal of SLFP battery cathode materials, the direct generation of SLFP battery cathode materials offers a promising approach that balances economic and environmental benefits. Consequently, the development of a strategy for LFP restoration that is capable of practical production use and higher performance remains a great challenge. These include the following:

Lack of economy and practicality

The more popular organic lithium salt offers the advantage of simultaneously providing a carbon source and lithium source. However, the high cost of organic lithium salt, coupled with the potential generation of carbon dioxide during their regeneration process poses environmental concerns. These factors present significant challenges to their large-scale industrial application. Most current research remains at the laboratory stage and is not easily scalable for industrial use. Thus, future research should focus on large-scale production and exploring more efficient and universal regeneration processes.

Repair of crystal structure

Indirect recycling and subsequent regeneration of LFP *via* high-temperature calcination produce cathode materials with enhanced crystal structure stability compared with some direct regeneration methods. These direct methods often involve low-temperature reduction for lithium replenishment and omit the annealing process, resulting in weaker crystal structure stability. Therefore, a significant challenge lies in balancing low energy consumption with the improvement in crystal structure stability. Therefore, balancing the low energy consumption and improving the stability of the crystal structure is also a major research focus.

Problems of impurities

During the recycling process, impurities such as copper and aluminum in the battery need to be effectively removed to ensure the purity of the recovered material and the safety of reuse. It is imperative to develop more refined separation techniques, such as magnetic separation and froth flotation, to enhance the efficiency of the separation processes and the purity of the recovered materials. Synchronous interfacial impurity removal and lithium replenishment could shorten the closed-loop battery material recycling process. However, the battery failure and regeneration mechanisms need deeper exploration.

Problems with the surface interface

The surface interface properties of battery materials are pivotal to their electrochemical performance; however, there is a paucity of research concerning LFP recycling. It is imperative for future investigations to focus on enhancing the surface interface properties of recycled materials to optimize their performance in secondary applications. Potential methodologies to achieve this enhancement may encompass surface coating, doping, or the development of specialized surface-interface structures.

The chemical reaction mechanism of the regeneration process is not well understood

The intercalation/expulsion kinetics of lithium ions during regeneration are affected by many factors. Most of the existing studies rely on empirical adjustment and lack an atomic-level simulation of the phase transition mechanism of $LiFePO_4 \rightarrow FePO_4 \rightarrow LiFePO_4$. It is difficult to form a regeneration process that can be accurately controlled.

Author contributions

Junhui Cai and Yanjuan Li wrote the original draft. Yiran Li and Shengnv Xu contributed to the preparation of figures and tables. Zhanzhan Wang and Jie Liu contributed to the review of typography and language. Shun Yang and Xiao Yan contributed to the review design and supervision.

Data availability

No primary research results, software or code have been included and no new data were generated or analysed as part of this review.

Conflicts of interest

There are no conflicts to declare.

Acknowledgements

This work was supported by National Natural Science Foundation of China (No. 52474439) and Natural Science Research of Jiangsu Higher Education Institutions of China (No. 24KJA480002 and 21KJA430003).

References

1 D. Larcher and J. M. Tarascon, *Nat. Chem.*, 2015, **7**, 19–29.
2 V. Anoopkumar, B. John and T. D. Mercy, *ACS Appl. Energy Mater.*, 2020, **3**, 9478–9492.
3 H. Kim, J. Hong, K.-Y. Park, H. Kim, S.-W. Kim and K. Kang, *Chem. Rev.*, 2014, **114**, 11788–11827.
4 R. A. Kerr, *Science*, 1998, **281**, 1128–1131.
5 S. Jenu, I. Deviatkin, A. Hentunen, M. Myllysilta, S. Viik and M. Pihlatie, *J. Energy Storage*, 2020, **27**, 101023.
6 T. M. Gür, *Energy Environ. Sci.*, 2018, **11**, 2696–2767.
7 Y. Chen, J. Qian, X. Hu, Y. Ma, Y. Li, T. Xue, T. Yu, L. Li, F. Wu and R. Chen, *Adv. Mater.*, 2023, **35**, 2212096.
8 D. Qin, L. Wang, X. Zeng, J. Shen, F. Huang, G. Xu, M. Zhu and Z. Dai, *Energy Storage Mater.*, 2023, **54**, 498–507.
9 B. L. Ellis, K. T. Lee and L. F. Nazar, *Chem. Mater.*, 2010, **22**, 691–714.
10 Y. Miao, P. Hynan, A. von Jouanne and A. Yokochi, *Energies*, 2019, **12**, 1074.
11 Y. Ding, Z. P. Cano, A. Yu, J. Lu and Z. Chen, *Electrochem. Energy Rev.*, 2019, **2**, 1–28.
12 Global EV Outlook 2024.
13 J. Weng and L. Peng, *Mater. Chem. Phys.*, 2022, **282**, 125997.
14 X.-G. Yang, T. Liu and C.-Y. Wang, *Nat. Energy*, 2021, **6**, 176–185.
15 N. Nitta, F. Wu, J. T. Lee and G. Yushin, *Mater. Today*, 2015, **18**, 252–264.
16 T. Zhao, H. Mahandra, R. Marthi, X. Ji, W. Zhao, S. Chae, M. Traversy, W. Li, F. Yu, L. Li, Y. Choi, A. Ghahreman, Z. Zhao, C. Zhang, Y. Kang, Y. Lei and Y. Song, *Chem. Eng. J.*, 2024, **485**, 149923.
17 M. Shan, C. Dang, K. Meng, Y. Cao, X. Zhu, J. Zhang, G. Xu and M. Zhu, *Mater. Today*, 2024, **73**, 130–150.
18 T. Yan, S. Zhong, M. Zhou, X. Guo, J. Hu, F. Wang, F. Zeng and S. Zuo, *Nanotechnol. Rev.*, 2020, **9**, 1586–1593.
19 H. Li, S. Xing, Y. Liu, F. Li, H. Guo and G. Kuang, *ACS Sustainable Chem. Eng.*, 2017, **5**, 8017–8024.
20 K. Liu, S. Yang, F. Lai, Q. Li, H. Wang, T. Tao, D. Xiang and X. Zhang, *Ionics*, 2021, **27**, 5127–5135.
21 Y. Chen, L. Wang, H. He, J. Li, Y. Li, R. Liu, D. Li and Z. He, *J. Mater. Sci.: Mater. Electron.*, 2020, **31**, 4083–4091.
22 M. Zhang, L. Wang, S. Wang, T. Ma, F. Jia and C. Zhan, *Small Methods*, 2023, **7**, e2300125.
23 G. Ji, J. Wang, Z. Liang, K. Jia, J. Ma, Z. Zhuang, G. Zhou and H. M. Cheng, *Nat. Commun.*, 2023, **14**, 584.
24 Y. Zou, J. Cao, H. Li, W. Wu, Y. Liang and J. Zhang, *Ind. Chem. Mater.*, 2023, **1**, 254–261.
25 J. Tang, H. Qu, C. Sun, X. Xiao, H. Ji, J. Wang, J. Li, G. Ji, X. Zhang, H. M. Cheng and G. Zhou, *Adv. Mater.*, 2025, e2420238.
26 T. Zhao, Y. Choi, C. Wu, Z. Zhang, C. Wang, D. Liu, W. Xu, H. Huang, X. Huo, W. Zhao, Z. Zhao and W. Li, *Sci. Total Environ.*, 2024, **957**, 177748.
27 T. Zhao, W. Li, M. Traversy, Y. Choi, A. Ghahreman, Z. Zhao, C. Zhang, W. Zhao and Y. Song, *J. Environ. Manage.*, 2024, **351**, 119670.
28 T. Zhao, H. Mahandra, R. Marthi, X. Ji, W. Zhao, S. Chae, M. Traversy, W. Li, F. Yu, L. Li, Y. Choi, A. Ghahreman, Z. Zhao, C. Zhang, Y. Kang, Y. Lei and Y. Song, *Chem. Eng. J.*, 2024, **485**, 149923.
29 P. Xu, Q. Dai, H. Gao, H. Liu, M. Zhang, M. Li, Y. Chen, K. An, Y. S. Meng, P. Liu, Y. Li, J. S. Spangenberger, L. Gaines, J. Lu and Z. Chen, *Joule*, 2020, **4**, 2609–2626.
30 S.-H. Luo, Y. Wang, Q. Liu, P. Li, Z. Wang, S. Yan and F. Teng, *J. Ind. Eng. Chem.*, 2024, **133**, 65–73.
31 D. Saju, J. Ebenezer, N. Chandran and N. Chandrasekaran, *Ind. Eng. Chem. Res.*, 2023, **62**, 11768–11783.
32 J. Yan, J. Qian, Y. Li, L. Li, F. Wu and R. Chen, *Adv. Funct. Mater.*, 2024, **34**, 495.
33 S.-Q. Jiang, X.-G. Li, Q. Gao, X.-J. Lyu, S. N. Akanyange, T.-T. Jiao and X.-N. Zhu, *Sep. Purif. Technol.*, 2023, **324**, 104015.
34 R. Malik, D. Burch, M. Bazant and G. Ceder, *Nano Lett.*, 2010, **10**, 4123–4127.
35 Y. Jin, T. Zhang and M. Zhang, *Adv. Energy Mater.*, 2022, **12**, 2201526.
36 T. Yang, D. Luo, A. Yu and Z. Chen, *Adv. Mater.*, 2023, **35**, 2203218.
37 X. Chen, S. Li, Y. Wang, Y. Jiang, X. Tan, W. Han and S. Wang, *Waste Manage.*, 2021, **136**, 67–75.
38 Q. Jing, J. Zhang, Y. Liu, W. Zhang, Y. Chen and C. Wang, *ACS Sustainable Chem. Eng.*, 2020, **8**, 17622–17628.

39 Y. Yang, Z. Liu, J. Zhang, Y. Chen and C. Wang, *J. Alloys Compd.*, 2023, **947**, 169660.
40 Y. Peng, C. Zhong, M. Ding, H. Zhang, Y. Jin, Y. Hu, Y. Liao, L. Yang, S. Wang, X. Yin, J. Liang, Y. Wei, J. Chen, J. Yan, X. Wang, Z. Gong and Y. Yang, *Adv. Funct. Mater.*, 2024, **34**, 2404495.
41 K. Fu, X. Li, K. Sun, H. Yang, L. Gong and P. Tan, *J. Power Sources*, 2024, **606**, 234568.
42 D. Wang, X. Wu, Z. Wang and L. Chen, *J. Power Sources*, 2005, **140**, 125–128.
43 H. Gabrisch, J. Wilcox and M. M. Doeff, *Electrochem. Solid-State Lett.*, 2008, **11**, A25.
44 R. Xu, H. Sun, L. S. de Vasconcelos and K. Zhao, *J. Electrochem. Soc.*, 2017, **164**, A3333.
45 I. Azzouz, R. Yahmadi, K. Brik and F. B. Ammar, *Electr. Eng.*, 2022, **104**, 27–43.
46 C. R. Birkl, M. R. Roberts, E. McTurk, P. G. Bruce and D. A. Howey, *J. Power Sources*, 2017, **341**, 373–386.
47 Y. Liu and J. Xie, *J. Electrochem. Soc.*, 2015, **162**, A2208.
48 H. Zheng, L. Chai, X. Song and V. Battaglia, *Electrochim. Acta*, 2012, **62**, 256–262.
49 P. Liu, J. Wang, J. Hicks-Garner, E. Sherman, S. Soukiazian, M. Verbrugge, H. Tataria, J. Musser and P. Finamore, *J. Electrochem. Soc.*, 2010, **157**, A499.
50 J. Deng, G. J. Wagner and R. P. Muller, *J. Electrochem. Soc.*, 2013, **160**, A487.
51 W. L. Chen, C. Chen, H. Xiao, C. W. Chen and D. Sun, *Molecules*, 2023, **28**, 144343.
52 J. Wang and X. Sun, *Energy Environ. Sci.*, 2012, **5**, 5163–5185.
53 D. Fu, W. Zhou, J. Liu, S. Zeng, L. Wang, W. Liu, X. Yu and X. Liu, *Sep. Purif. Technol.*, 2024, **342**, 127069.
54 H. Zhou, Z. Luo, S. Wang, X. Ma and Z. Cao, *Sep. Purif. Technol.*, 2023, **315**, 6057–6066.
55 X. Qiu, B. Zhang, Y. Xu, J. Hu, W. Deng, G. Zou, H. Hou, Y. Yang, W. Sun, Y. Hu, X. Cao and X. Ji, *Green Chem.*, 2022, **24**, 2506–2515.
56 Y. Xu, X. Qiu, B. Zhang, A. Di, W. Deng, G. Zou, H. Hou and X. Ji, *Green Chem.*, 2022, **24**, 7448–7457.
57 X. Chen, L. Yuan, S. Yan and X. Ma, *Chem. Eng. J.*, 2023, **471**, 123742.
58 J. Zhang, J. Zou, D. He, W. Hu, D. Peng, Y. Li, Z. Zhao, S. Wang, P. Li, S. Su, K. Ma and X. Wang, *Green Chem.*, 2023, **25**, 6057–6066.
59 F. Sun, M. Gao, W. Jiao, L. Qi, Z. He, H. Zhang, Y. Cao, D. Song and L. Zhang, *J. Alloys Compd.*, 2023, **965**, 127069.
60 B. Chen, M. Liu, S. Cao, G. Chen, X. Guo and X. Wang, *Mater. Chem. Phys.*, 2022, **279**, 14323–14334.
61 J. Chen, Q. Li, J. Song, D. Song, L. Zhang and X. Shi, *Green Chem.*, 2016, **18**, 2500–2506.
62 X. Li, M. Wang, Q. Zhou, M. Ge, M. Zhang, W. Liu, Z. Shi, H. Yue, H. Zhang, Y. Yin and S.-T. Yang, *ACS Mater. Lett.*, 2024, **6**, 640–647.
63 J. Wang, S. Ji, Q. Han, F. Wang, W. Sha, D. Cheng, W. Zhang, S. Tang, Y.-C. Cao and S. Cheng, *J. Mater. Chem. A*, 2024, **12**, 15311–15320.
64 R. Fu, P.-S. Zhang, Y.-X. Jiang, L. Sun and X.-H. Sun, *Chemosphere*, 2023, **311**, 136993.
65 G. Nair, B. Soni and M. Shah, *Groundw. Sustain. Dev.*, 2023, **23**, 100980.
66 S. Tian, Y. Cao, L. Dong, P. Shi, R. Li, Y. Jin, Y. Tu, C. Du, Z. Ren and Z. Zhou, *J. Environ. Chem. Eng.*, 2024, **12**, 112871.
67 B. Zhang, L. He, J. Wang, Y. Liu, X. Xue, S. He, C. Zhang, Z. Zhao, L. Zhou, J. Wang and Z. L. Wang, *Energy Environ. Sci.*, 2023, **16**, 3873–3884.
68 Z. Liu, C. Zhang, M. Ye, H. Li, Z. Fu, H. Zhang, G. Wang and Y. Zhang, *ACS Appl. Energy Mater.*, 2022, **5**, 14323–14334.
69 C. Yang, J.-L. Zhang, Q.-K. Jing, Y.-B. Liu, Y.-Q. Chen and C.-Y. Wang, *Int. J. Miner., Metall. Mater.*, 2021, **28**, 1478–1487.
70 Q. Jing, J. Zhang, Y. Liu, W. Zhang, Y. Chen and C. Wang, *ACS Sustainable Chem. Eng.*, 2020, **8**, 17622–17628.
71 X. Song, Y. Xu, L. Cheng, T. Ren, B. Cai, D. Yang, J. Chen, T. Liang, R. Huang, E. H. Ang, X. Liao, B. Ge and H. Xiang, *J. Energy Storage*, 2024, **82**, 110578.
72 T. Ren, B. Zou, B. Cai, T. Liang, J. Chen, R. Huang, D. Yang, H. Xiang, E. H. Ang and X. Song, *Waste Manage.*, 2024, **183**, 209–219.
73 Z. Wang, H. Xu, Z. Liu, M. Jin, L. Deng, S. Li and Y. Huang, *J. Mater. Chem. A*, 2023, **11**, 9057–9065.
74 T. Ouaneche, M. Courty, L. Stievano, L. Monconduit, C. Guéry, M. T. Sougrati and N. Recham, *J. Power Sources*, 2023, **579**, 233248.
75 H. Sun, X. Li, B. Wu, K. Zhu, Y. Gao, T. Bao, H. Wu and D. Cao, *Chin. Chem. Lett.*, 2024, 110041.
76 S. Hao, Y. Lv, Y. Zhang, S. Liu, Z. Tan, W. Liu, Y. Xia, W. Yin, Y. Liao, H. Ji, Y. Kong, Y. Shao, Y. Huang and L. Yuan, *Energy Environ. Sci.*, 2025, **18**, 3750–3760.
77 C. Feng, Y. Cao, L. Song, B. Zhao, Q. Yang, Y. Zhang, X. Wei, G. Zhou and Y. Song, *Angew. Chem., Int. Ed.*, 2025, **64**, e202418198.
78 X. Zhong, X. Mao, W. Qin, H. Zeng, G. Zhao and J. Han, *Waste Manage.*, 2023, **156**, 236–246.
79 X. Song, B. Zou, J. Wang, T. Ren, B. Cai, B. Ge, J. Chen, T. Liang, E. H. Ang, X. Liao and H. Xiang, *Mater. Today Chem.*, 2024, **38**, e202409929.
80 M. Xiao, X. Fu, M. Chen, M. Ye, C. Zhu, F. Wan and X. Guo, *ACS Appl. Mater. Interfaces*, 2025, **17**, 12199–12207.
81 M. Xiao, X. Fu, M. Chen, M. Ye, C. Zhu, F. Wan and X. Guo, *ACS Appl. Mater. Interfaces*, 2025, **17**, 12199–12207.
82 Y. Cao, J. Li, D. Tang, F. Zhou, M. Yuan, Y. Zhu, C. Feng, R. Shi, X. Wei, B. Wang, Y. Song, H.-M. Cheng and G. Zhou, *Adv. Mater.*, 2024, **36**, 2414048.
83 Z. Jiang, J. Sun, P. Jia, W. Wang, Z. Song, X. Zhao and Y. Mao, *Sustainable Energy Fuels*, 2022, **6**, 2207–2222.
84 J. Sun, Z. Jiang, P. Jia, S. Li, W. Wang, Z. Song, Y. Mao, X. Zhao and B. Zhou, *Waste Manage.*, 2023, **158**, 125–135.
85 K. Jia, J. Ma, J. Wang, Z. Liang, G. Ji, Z. Piao, R. Gao, Y. Zhu, Z. Zhuang, G. Zhou and H. M. Cheng, *Adv. Mater.*, 2023, **35**, e2208034.

86 Y. Gou, C. Qi, R. Li, X. Liu, Z. Zhou, M. Zhang, Q. Sun, L. Song and Y. Jin, *Electrochim. Acta*, 2024, **488**, 169660.
87 G. Ji, J. Wang, Z. Liang, K. Jia, J. Ma, Z. Zhuang, G. Zhou and H. M. Cheng, *Nat. Commun.*, 2023, **14**, 584.
88 D. Peng, X. Wang, S. Wang, B. Zhang, X. Lu, W. Hu, J. Zou, P. Li, Y. Wen and J. Zhang, *Green Chem.*, 2022, **24**, 4544–4556.
89 D. Yang, Z. Fang, Y. Ji, Y. Yang, J. Hou, Z. Zhang, W. Du, X. Qi, Z. Zhu, R. Zhang, P. Hu, L. Qie and Y. Huang, *Angew. Chem., Int. Ed. Engl.*, 2024, e202409929, DOI: **10.1002/anie.202409929**.
90 S. Zhou, J. Du, X. Xiong, L. Liu, J. Wang, L. Fu, J. Ye, Y. Chen and Y. Wu, *Green Chem.*, 2022, **24**, 6278–6286.
91 Y. Yang, J. Zhang, H. Zhang, Y. Wang, Y. Chen and C. Wang, *Energy Storage Mater.*, 2024, **65**, 103081.
92 D. Yang, Z. Fang, Y. Ji, Y. Yang, J. Hou, Z. Zhang, W. Du, X. Qi, Z. Zhu, R. Zhang, P. Hu, L. Qie and Y. Huang, *Angew. Chem., Int. Ed.*, 2024, **63**, e202409929.
93 S. Zhou, J. Du, X. Xiong, L. Liu, J. Wang, L. Fu, J. Ye, Y. Chen and Y. Wu, *Green Chem.*, 2022, **24**, 6278–6286.
94 X. Zhao, H. Chen, H. Wu, Y. Zhao and J. Luo, *ACS Nano*, 2024, **18**, 21125–21134.
95 B. Wang, Y. Li, X. Zhu, F. Guo, D. Zhang and H. Wang, *New J. Chem.*, 2024, **48**, 10949–10960.
96 Y. Yang, Z. Liu, J. Zhang, Y. Chen and C. Wang, *J. Alloys Compd.*, 2023, **947**, 169660.
97 Y. Zou, J. Cao, H. Li, W. Wu, Y. Liang and J. Zhang, *Ind. Chem. Mater.*, 2023, **1**, 254–261.
98 B. Chen, M. Liu, S. Cao, H. Hu, G. Chen, X. Guo and X. Wang, *J. Alloys Compd.*, 2022, **924**, 166487.